



Electronic structure of Pt/HfO₂ interface with oxygen vacancy

Eunae Cho, Seungwu Han *

Department of Physics, Ewha Womans University, Seoul 120-750, Republic of Korea

ARTICLE INFO

Article history:

Received 15 October 2008

Received in revised form 8 July 2009

Accepted 4 November 2009

Available online 10 November 2009

Keywords:

First-principles calculation

Metal–oxide interface

Oxygen vacancy

Charge transfer

ABSTRACT

Using first-principles calculations, we study the electronic structures of Pt/HfO₂ interface in the presence of oxygen vacancy. The energetics and charge transfer are examined when the oxygen vacancy is at various distances from the interface. It is found that the oxygen vacancy is strongly attracted to the interface and the charge transfer decreases monotonically as the vacancy moves away from the interface, albeit the amount of charge transfer is small. The charge transfer results in the decrease of the effective work function of Pt, consistent with the vacancy mechanism to explain the shift in the flat-band voltage.

© 2009 Published by Elsevier B.V.

1. Introduction

With the aggressive scaling of traditional metal–oxide–semiconductor field effect transistor (MOSFET), the leakage current through the gate stack becomes significant due to the quantum tunneling. To cope with these problems, SiO₂ used as gate insulators is being replaced by high dielectric constant (high-*k*) oxide. The tunneling current can be suppressed by increasing the physical thickness of the gate oxide. Among various materials explored to date, Hf-based high-*k* materials are considered to be most promising since they satisfy various technical requirements. However, the replacement gate oxides gave rise to several technical problems such as the degradation of carrier mobility, material stability under annealing, and the depletion of poly-Si gates [1]. It has been known that these problems can be overcome by switching the material for gate electrodes from poly-Si to metals. This gate metals are chosen such that the Fermi level is aligned near the conduction (valence) edge of Si for n-type (p-type) MOSFETs. The metal/high-*k* gate stack has many advantages such as higher physical thickness of dielectric film, a good stability, and high electron mobility. In particular, the metal gates are known to overcome charge depletion and the Fermi level pinning.

The introduction of high-*k* in combination with metal gates can be marked as a most radical shift ever attempted by the semiconductor industry. Consequently, there exist several issues to be addressed to further improve the reliability of devices based on high-*k* dielectrics. For instance, it has been observed that the flat-band voltage (V_{fb}) shifts after post-deposition annealing [1–3]. This

is especially pronounced for metal gates with high work functions used in p-type MOSFET. The V_{fb} shifts are interpreted as the change in the work function of metal gates interfaced with high-*k* materials. The electrically active oxygen vacancies are receiving most attention among various origins for the V_{fb} shifts [1,4–9]. Although the defect formation energies of the oxygen vacancies in HfO₂ is relatively high, they can be easily generated in actual devices with the help of the oxidation of underlying silicon [4,7]. It was proposed that the charge transfer between the oxygen vacancy and metal electrode can cause a large shift in the band offset. In the previous publication, we have shown that the oxygen vacancies tend to segregate at the interface, in particular for the metals with large work functions [10]. In this work, we provide detailed analysis on the Pt/HfO₂ interface with oxygen vacancies at various positions from the interface. As a previous literature on metal–oxide interface, the interface between Mo and HfO₂ was investigated in Ref. [11]. In particular, the oxygen vacancy created in the form of an extended Schottky pair was studied and a shift in the Fermi level was observed. Compared to this literature, the present study will report on the systematic analysis on the energetics of the oxygen vacancy in the various positions from the interface.

2. Computational methods and model system

We employ first-principles methods using Vienna *Ab-initio* Simulation Package (VASP) throughout this work [12]. The energy cutoff for a plane-wave expansion is chosen to be 500 eV and the *k*-points are sampled on $5 \times 5 \times 1$ meshes for Pt/HfO₂ interfaces. The projector-augmented-wave (PAW) pseudo-potentials [13] are used to describe electron–ion interactions and the exchange–correlation energies between electrons are described within the

* Corresponding author.

E-mail address: hansw@ewha.ac.kr (S. Han).

local density approximation (LDA) [14]. The density of states is smeared by Gaussian functions with a width of 0.02 eV. The atomic positions are relaxed until the Hellmann–Feynman force on each atom is reduced to within 0.02 eV/Å. This choice of computational parameters ensures the convergence of structural parameters and total energies within 0.01 Å and 10 meV/atom, respectively.

As a model system, we choose (1 × 1) unit cell of monoclinic-HfO₂ (0 0 1) surface interfaced with (2 × √3) unit cell of Pt metal along (1 1 1) direction. It is noted that the monoclinic and amorphous HfO₂ are similar in electronic structure and local bonding configurations [15]. The calculated work function of Pt metal is 6.08 eV and therefore Pt metal represents the metal electrode used in p-type MOSFET. The vacuum with a length of 12 Å is inserted between repeated metal–insulator slab models. To match the lateral periodicity between HfO₂ and Pt metal, the lattice parameters of Pt are matched to those of HfO₂ (5.020 × 5.120 Å²). This reflects the experimental condition that metal electrodes are deposited on top of grown HfO₂ films. The lattice parameters of Pt are expanded by 8.0% and −7.2% along x and y directions, respectively. The strain effects are negligible as discussed in Ref. [10] with further details.

It is very difficult to find the “truly” stable structure for the low-symmetry interfacial structure formed between metal and monoclinic-HfO₂. To find a reasonable interfacial structure within our computational resource, we use a systematic approach as follows; the lateral unit area is divided into a 5 × 5 grid with ∼1 Å between grid points. The lateral position of metal layers is shifted over the grid points and relaxed subsequently. Among 25 relaxed structures, the one with the lowest total energy was chosen and oxygen vacancies are introduced. The energy differences between 25 structures are 0.5 eV per unit supercell. In particular, the minimum-energy structure agrees very well with that in Ref. [16], where the simulated annealing technique was used to optimize the interfacial structure. The unit cell of model structure is shown in Fig. 1a.

3. Interface energetics in the presence of oxygen vacancy

Firstly, we investigate how the total energy changes as an oxygen vacancy approaches the Pt/HfO₂ interface. An oxygen vacancy is introduced by removing a fourfold coordinated oxygen atom from one of 1–8 sites in Fig. 1a. The formation energy is slightly lower for a fourfold atom compared to the threefold coordinated oxygen atom [17]. Before discussing the energetics, we validate the vacancy density in our model system. Although there is no experimental data on the density of the oxygen vacancy generated from post-deposition annealing, theoretical analysis in Ref. [4] indicates that it could be as high as 10²⁰–10²¹ cm^{−3} for p metals. Assuming that the thickness of HfO₂ is 10 nm, this corresponds to the areal vacancy density of 1–10 nm^{−2}. If there exists one vacancy per (1 × 1) interface, the areal density is 4 nm^{−2}, which is within the theoretical range. Therefore, the supercell size in our model is appropriate to study the effects of oxygen vacancies on the interface between HfO₂ and p metals, which is a primary interest in this work. To inspect the effect of the supercell size, we also calculated on the expanded model with the supercell length doubled in one direction [from (1 × 1) to (1 × 2)]. It is found that the defect formation energy (see below) of the oxygen vacancy close to the interface increases only by 0.4%. Therefore, even if the vacancy density is smaller than our estimates by an order, it is expected that the main conclusions would not change.

Fig. 1b shows the defect formation energy with respect to the bulk value $\Delta\Omega_f = \Omega_f - \Omega_{f,bulk}$ for Pt/HfO₂ interface. For the purpose of analysis, two types of calculations are shown separately. In “un-relaxed” calculations, atomic positions are frozen at their equilibrium positions determined for the vacancy-free interface. In contrast, all atoms are allowed to optimize in “relaxed” results. For

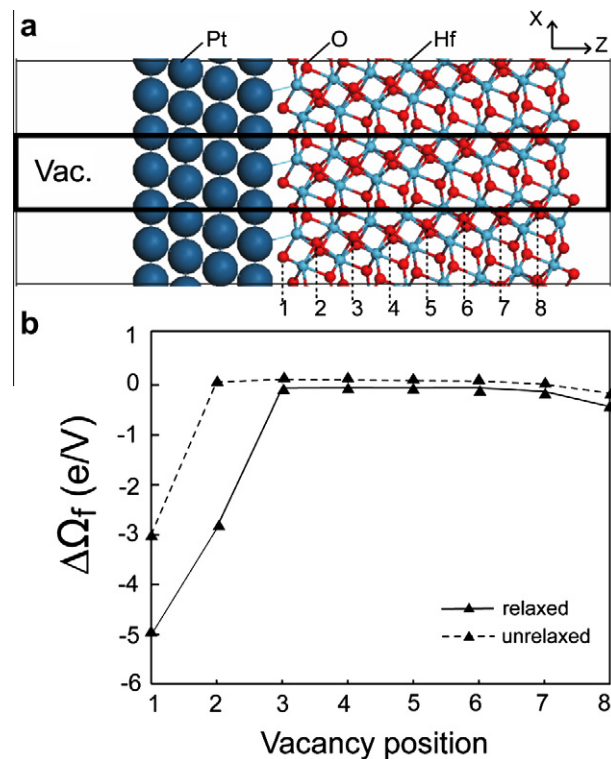


Fig. 1. (a) Unit cell of the model structure. The oxygen vacancy positions are noted as 1–8. (b) Defect formation energy ($\Delta\Omega_f$) of the oxygen vacancy in Pt/HfO₂ interface with respect to the bulk value. The “relaxed” data is the energy with all atomic positions are fully relaxed while “un-relaxed” data are obtained with atoms fixed at the equilibrium positions for clean Pt/HfO₂ interface (without oxygen vacancy).

both types of calculations, total energies remain almost constant inside the slab but they drop sharply when the vacancy is right next to the metal layers. On the other hand, when ions are allowed to relax, the binding energies further increase by ∼2.0 eV due to the formation of additional Pt–Hf bonds at the interface regions. Such a strong binding of oxygen vacancy to the interface was attributed to the change in the transition level (the position of the Fermi level at which the charge state of the oxygen vacancy changes) of the oxygen vacancy and formation of interfacial bonding [10].

4. Charge transfer and band offset

The classical model of vacancy–metal interactions is based on the electrostatic interaction between ionized vacancies and induced image charges. To estimate the charge state of the oxygen vacancy in our model systems, we calculate the charge difference defined as $\Delta\rho = \rho(\text{Pt}/\text{HfO}_2) - \rho(\text{Pt}) - \rho(\text{HfO}_2)$. In calculating the charge density of separate systems, the atomic positions are frozen to those in the interface structure. Fig. 2a shows $\Delta\rho$ when the oxygen vacancy is close to the metal layer (about 18 Å as marked by the dashed line) while Fig. 2b shows the charge difference when the oxygen vacancy is in the middle of the oxide slab. The overall magnitude of charge difference in Fig. 2a is larger than that in Fig. 2b. This indicates that the redistribution of electrons is more significant when the vacancy is right to the metal layer. It is also found that the charge redistribution in the metallic side is oscillating at small scale, which means that the density of free electrons is perturbed up to ∼7 Å inside the metal layer.

The charge transfer around the vacancy in the middle of slab (dashed circle in Fig. 2b) is rather small. The sign of the charge

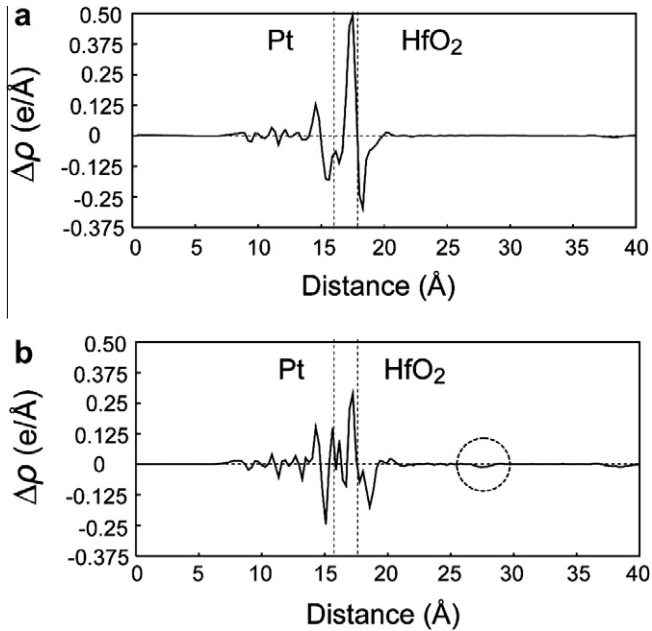


Fig. 2. The charge difference for Pt/HfO₂ interfaces: $\Delta\rho = \rho(\text{Pt}/\text{HfO}_2) - \rho(\text{Pt}) - \rho(\text{HfO}_2)$ (a) with oxygen vacancy at the position 1, (b) with oxygen vacancy at the position 5 (see Fig. 1a). The vertical dashed lines indicate the position of Pt and HfO₂ layer closest to the interface.

transfer is negative and therefore a fraction of electron is transferred from HfO₂ to Pt. The inspection of spatial distribution of $\Delta\rho$ around the vacancy site confirms that it is derived from the defect level. This is because the defect level of the oxygen vacancy in HfO₂ is above the Fermi level of Pt before forming the interface. The charge differences show a similar shape around defect region when the vacancy position is 2–8. In Fig. 3, we calculate the amount of charge transfer per unit interface cell for vacancy positions 1–8. It is found that the charge transfer decreases monotonically as the oxygen vacancy moves away from the interface; when the vacancy is on 1 and 2 sites near the interface, the charge difference is about $0.1e$ but it decreases to $0.02e$ at the position 5. Even though the charge transfer is small, the large lateral density results in a significant change in the band offset as will shown in the below. The oxygen vacancy is known to exist in five different charge states from -2 to $+2$. In the present study, the charge state of the oxygen vacancy is self-consistently determined through the charge transfer between the metal and the oxygen vacancy. The small values of the charge transfer in Fig. 3 imply that the oxygen vacancy is close to the neutral state.

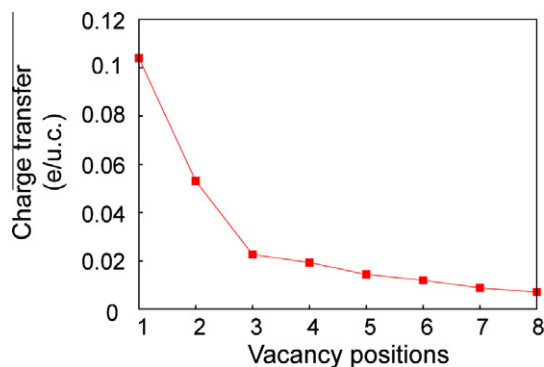


Fig. 3. The amount of charge transfer per unit interface cell when vacancies are at various positions.

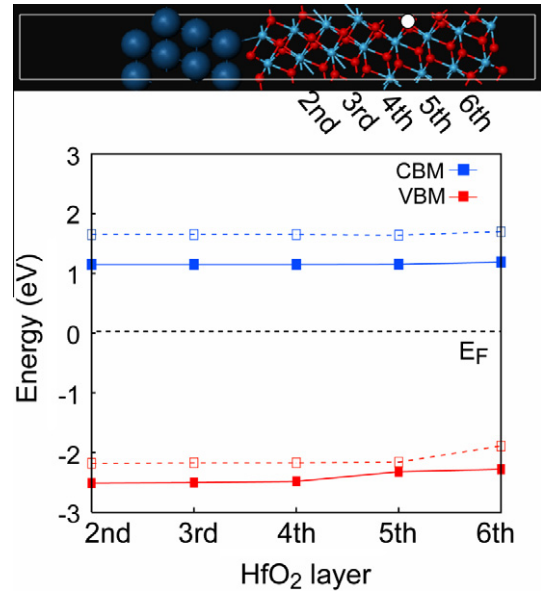


Fig. 4. The layer-by-layer position of valence and conduction edges with respect to the metal Fermi level. The dashed lines represent results for clean interface while the solid lines are results for the vacancy at 5th layer of HfO₂. This position is indicated as a white disk at the top figure.

In order to investigate the band offset, we calculate the valence band maximum (VBM) and conduction band minimum (CBM) with respect to the Fermi level using partial density of states (PDOS) for interfaces [18]. In Fig. 4, band edges are shown in a layer-by-layer way. The dashed lines show the energy position of VBM and CBM when there is no oxygen vacancy. From the figure, the conduction band offset is 1.7 eV. On the other hand, the solid lines are results with the oxygen vacancy at the position 5. It is found that the oxygen vacancy effectively lowers the work function of Pt by 0.6 eV. This is consistent with the vacancy mechanism to explain the shift of flat-band voltage after annealing [1]. We note that the layer-by-layer position of VBM and CBM in Fig. 4 shows an interesting behavior. That is to say, the band bending inside HfO₂ slab is almost negligible. This is due to the small charge transfer and high dielectric constant of HfO₂. This also implies that the shift in the band offset and effective work function is induced by the charge redistribution right at the interface, rather than throughout the HfO₂ slab up to the vacancy site as implied in the typical schematic model [1].

5. Conclusions

In summary, we have carried out first-principles calculations on the Pt/HfO₂ interface in the presence of the oxygen vacancy. We analyzed the energetics and the charge transfer as the vacancy moves inside the oxide slab. It was found that the oxygen vacancy is strongly attracted to the interface and the charge transfer decreases monotonically as the vacancy moves away from the interface, although the amount of charge transfer is rather small. This charge transfer resulted in the decrease of the effective work function of Pt, consistent with the vacancy mechanism to explain the shift in the flat-band voltage and the Fermi level pinning.

Acknowledgements

This work was supported by the System IC2010 program and the Quantum Metamaterials Research Center (Grant No. R11-2008-053-03001-0).

References

- [1] E.P. Gusev, V. Narayanan, M.M. Frank, *IBM J. Res. Dev.* 50 (2006) 387.
- [2] S.C. Song, C.S. Park, J. Price, C. Burham, R. Choi, H.H. Tseng, B.H. Lee, R. Jammy, *IEDM Tech. Dig.* (2007) S13.3.
- [3] H.Y. Yu, C. Ren, Y.C. Yeo, J.F. Kang, X.P. Wang, H.H.H. Ma, M.F. Li, D.S.H. Chan, D.L. Kwong, *IEEE Electron Dev. Lett.* 25 (2004) 337.
- [4] J. Robertson, O. Sharia, A.A. Demkov, *Appl. Phys. Lett.* 91 (2007) 132912.
- [5] S. Guha, V. Narayanan, *Phys. Rev. Lett.* 98 (2007) 196101.
- [6] J.K. Schaeffer, L.R.C. Fonseca, S.B. Samavedam, Y. Liang, P.J. Tobin, B.E. White, *Appl. Phys. Lett.* 85 (2004) 1826.
- [7] Y. Akasaka, G. Nakamura, K. Shiraishi, N. Umezawa, K. Yamabe, O. Ogawa, M. Lee, T. Amiaka, T. Kasuya, H. Watanabe, T. Chikyow, F. Ootsuka, Y. Nara, K. Nakamura, *Jpn. J. Appl. Phys.* 45 (2006) L1289.
- [8] H. Takeuchi, H.Y. Wong, D. Ha, T.-J. King, *IEDM Tech. Dig.* (2004) 829.
- [9] D. Lim, R. Haight, M. Copel, E. Cartier, *Appl. Phys. Lett.* 87 (2005) 072902.
- [10] E. Cho, B. Lee, C.-K. Lee, S. Han, S.-H. Jeon, B.-H. Park, *Appl. Phys. Lett.* 92 (2008) 233118.
- [11] A.A. Demkov, *Phys. Rev. B* 74 (2006) 085310.
- [12] G. Kresse, J. Hafner, *Phys. Rev. B* 47 (1993) 558(R), 49 (1994) 14251.
- [13] P.E. Blöchl, *Phys. Rev. B* 50 (1994) 17953.
- [14] D.M. Ceperley, B.J. Alder, *Phys. Rev. Lett.* 45 (1980) 566.
- [15] X. Zhao, D. Ceresoli, D. Vanderbilt, *Phys. Rev. B* 71 (2005) 085107.
- [16] A.V. Gavrikov, A.A. Knizhnik, A.A. Bagatur'yants, B.V. Potapkin, L.R.C. Fonseca, M.W. Stoker, J. Schaeffer, *J. Appl. Phys.* 101 (2007) 014310.
- [17] A.S. Foster, F. Lopez Gejo, A.L. Shluger, R.M. Nieminen, *Phys. Rev. B* 65 (2002) 174117.
- [18] S.H. Jeon, B. Park, J. Lee, B. Lee, S. Han, *Appl. Phys. Lett.* 89 (2006) 042904.